ACSNANO

www.acsnano.org

ARTICLE

# Triboelectric Nanogenerator for Ocean Wave Graded Energy Harvesting and Condition Monitoring

Yuhong Xu,[⊥] Weixiong Yang,[⊥] Xiaohui Lu,[⊥] Yanfei Yang, Jianping Li, Jianming Wen,* Tinghai Cheng,* and Zhong Lin Wang*

Cite This: https://doi.org/10.1021/acsnano.1c05685

Read Online

ACCESS | Metrics & More | Article Recommendations | Supporting Information

**ABSTRACT:** **Using triboelectric nanogenerators (TENGs) to harvest blue energy in the ocean is advanced technology at present. In wave environments, the wave magnitude is constantly changing, so designing a TENG that can adjust the energy harvesting ability is necessary. Herein, a graded energy harvesting triboelectric nanogenerator (GEH-TENG) is fabricated, in which double generation units can operate in different transmission states to adapt to wave changes. Under small waves, the GEH-TENG is in the primary transmission state. Once waves are large enough, it enters the secondary transmission state, realizing graded energy harvesting to enhance power generation performance. Experiments show that when the input frequency is 1.0 Hz and the amplitude is 120 mm, the GEH-TENG can generate 0.7 mJ of energy in a single operation cycle, which is 2.3 times of it without grading. Moreover, it can be placed on the shore to monitor ocean wave conditions. An idea of graded energy harvesting is proposed in this study, and the proposal provides useful guidance for practical applications of TENGs in ocean wave condition monitoring.**

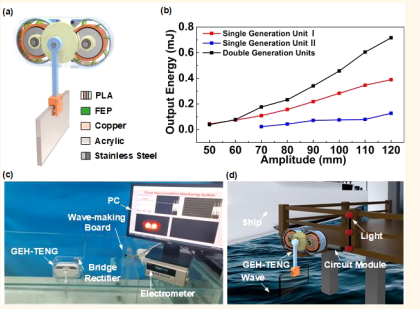


**KEYWORDS:** *triboelectric nanogenerator, ocean wave, graded energy harvesting, double generation units, condition monitoring*

The development and utilization of ocean energy have doubtless become an important means to solve the increasingly severe energy shortage problem.[1−3] Wave energy, as one of the main forms of ocean energy, is a reserve-abundant and widely distributed renewable energy source.[4−6] Therefore, realizing the large-scale utilization of wave energy will inevitably bring about the adjustment of global energy structure, thus solving the energy crisis. Currently, the method commonly employed in ocean energy harvesting is based on electromagnetic generators (EMGs).[7−9] While the EMG has a high energy harvesting efficiency in high-frequency conditions, it is weak in low-frequency conditions.[10−13] In most situations, wave motion involves low frequencies, so actively exploring approaches to harvesting wave energy is gaining a particular urgency.

Wang's group proposed triboelectric nanogenerators (TENGs) in 2012, which use displacement current as the driving force to convert mechanical energy into electric power/signal.[14−17] TENGs have shown a bright prospect in the fields of micro/nano power sources,[18−20] self-powered sensing,[21−23] blue energy,[24−28] and high voltage power sources.[29−31] Compared with EMGs, the biggest advantage of TENGs is that they are more suitable for harvesting mechanical energy widely existing in nature in low-frequency environments, and they also have outstanding advantages such as high power density, light weight, and extensive material selection range.[32−34] According to the inherent characteristics of wave low-frequency motion, the harvesting of wave energy using TENGs has gradually become a research hotspot. The time-varying characteristics of waves in the natural environment are obvious, and the magnitude of waves is constantly changing.[35] Therefore, to effectively harvest the ever-changing small waves and large waves, the ability of TENGs to harvest waves needs to be adjusted according to their changes, to effectively improve the output performance.

In this paper, a graded energy harvesting triboelectric nanogenerator (GEH-TENG) is proposed, which mainly consists of an outer shell, a pendulum, a graded transmission unit, and double generation units. When excitations of external waves are small, the swing angle of the pendulum is small, and

Received: July 5, 2021
Accepted: September 21, 2021

Downloaded via BEIJING INST NANOENERGY NANOSYSTEMS on September 23, 2021 at 15:35:39 (UTC).
See https://pubs.acs.org/sharingguidelines for options on how to legitimately share published articles.

ACS Publications

© XXXX American Chemical Society

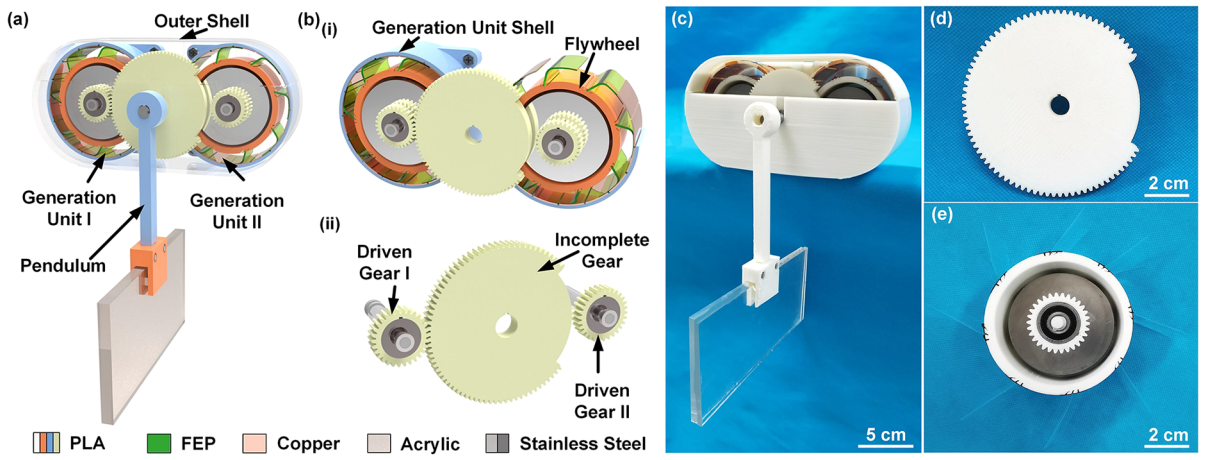


**Figure 1. Triboelectric nanogenerator for graded energy harvesting (GEH-TENG): (a) overall structure of the fabricated device, (b) structure details, (c) photo of a prototype, (d, e) components of the prototype.**

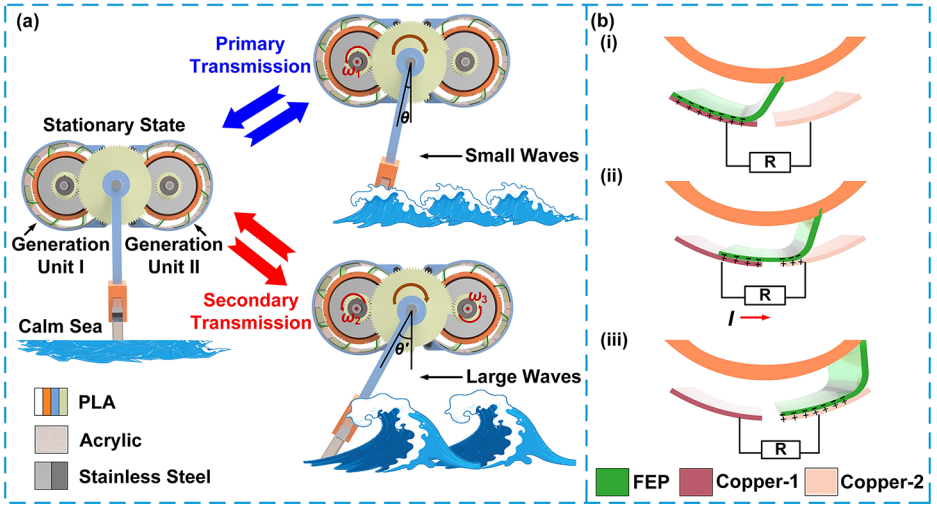


**Figure 2. Schematic of the working principle of the GEH-TENG: (a) different wave states and (b) power generation principles.**

the GEH-TENG is in a primary transmission state. When these excitations increase gradually, the swing angle of the pendulum increases until it exceeds a threshold value. Meanwhile, the GEH-TENG is in a secondary transmission state. In this period, the capability of the GEH-TENG in harvesting wave energy effectively improves. The wave magnitude needed to reach the threshold can be adjusted through the setting of intrinsic parameters. Experiments show that in a single cycle of operation, when the input frequency is 1.0 Hz and the amplitude is 120 mm, the GEH-TENG with double generation units can generate an output energy of 0.7 mJ, which is 2.3 times of it without grading; the peak power is calculated to be 4.6 mW. Furthermore, ocean wave conditions are monitored in a simulated wave environment, demonstrating its capability in practical applications. This work reports the idea of grading energy harvest, which provides effective guidance for the design and application of TENGs to harvest natural mechanical energy.

## RESULTS AND DISCUSSION

**Structural Design and Operation Principle.** The overall structure of the graded energy harvesting triboelectric nanogenerator (GEH-TENG) mainly comprises an outer shell, a pendulum, generation units I and II, and a graded transmission unit (Figure 1a). Generation unit I consists of a flywheel with eight flexible fluorinated ethylene propylene (FEP) films and a generation unit shell with sixteen copper electrodes attached to the inner wall [Figure 1b(i)]. The overall structure of generation unit II is the same as that of generation unit I. The graded transmission unit includes an incomplete gear, a driven gear I, and a driven gear II [Figure 1b(ii)]. To ensure that the flywheel always rotates unidirectionally, one-way clutches are installed on the driven gears I and II. The whole prototype of the GEH-TENG is illustrated in Figure 1c; Figure 1d and e show details of the incomplete gear and flywheel.

The working state of the GEH-TENG depends on the magnitude of the ambient input wave (Figure 2a). When the water surface is calm, the GEH-TENG is in a stationary state; there is no electric output signal. When a small wave impacts the pendulum, the GEH-TENG enters a primary transmission state. The pendulum swings through a small angle and drives the incomplete gear to rotate through the same angle. The incomplete gear drives the driven gear I to rotate, thereby generation unit I generates electric signals. During the whole process, the swing angle of the pendulum is small and the incomplete gear is unable to make driven gear II rotate. Under these conditions, generation unit II does not provide electric power.


https://doi.org/10.1021/acsnano.1c05685
ACS Nano XXXX, XXX, XXX−XXX

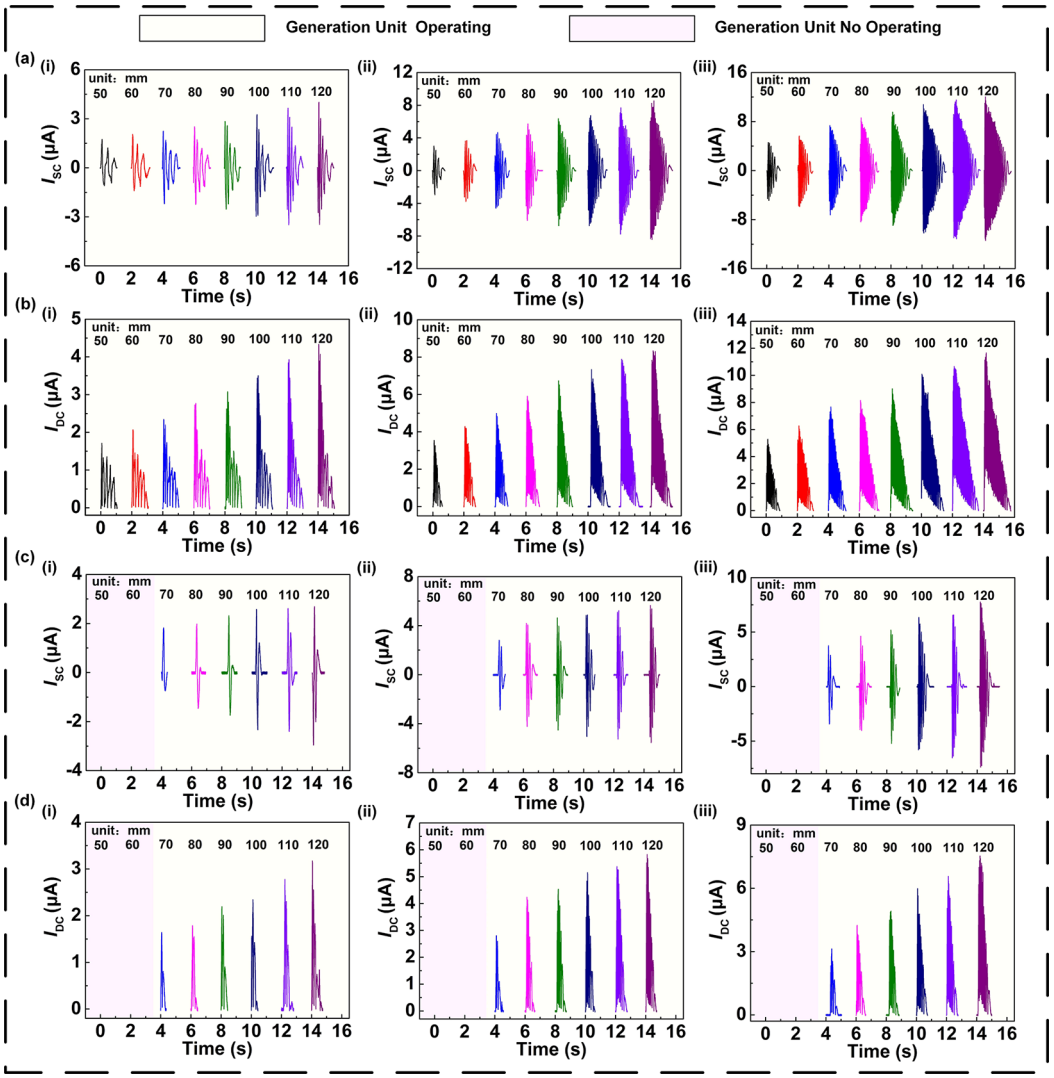


**Figure 3. Short-circuit current and direct-current comparison of the GEH-TENG under different input amplitudes and input frequencies of 0.5, 1.0, and 1.5 Hz with (a, b) only generation unit I and (c, d) only generation unit II.**

If the wave is sufficiently large, the swing angle of the pendulum exceeds the threshold value of the GEH-TENG. The threshold value is one-half of the incomplete angle of the incomplete gear. Simultaneously, the incomplete gear rotates to the position of the driven gear II. The GEH-TENG then enters its secondary transmission state, in which generation unit II combines its output with that of generation unit I, thereby achieving graded energy harvesting. In a small wave environment, the GEH-TENG is always in the primary transmission state, in which the initial torque is small and thus easily activated. In a large wave environment, the two generation units operate cooperatively to improve the output performance.

Figure 2b shows the power generation principles of the GEH-TENG. Because FEP and copper have opposite electronegativity, FEP can more easily obtain electrons than copper.[36,37] In the initial flywheel static state, copper-1 overlaps with the flexible FEP film, which carries electrons. From the law of charge conservation, copper-1 carries positive charges of equal number [Figure 2b(i)]. When the flywheel starts to rotate, the flexible FEP film on the flywheel gradually moves from copper-1 to copper-2. In this process, because of the potential difference, the positive charge on copper-1 is transferred to copper-2, generating a current in the external circuit accordingly [Figure 2b(ii)]. While the flywheel continues to rotate, the flexible FEP film completely overlaps with copper-2. All positive charges from copper-1 are transferred to copper-2, and hence charge equilibrium returns [Figure 2b(iii)]. The whole process repeats while the flywheel rotates, then a current is continuously present in the external circuit. To show the electron transfer process better, COMSOL Multiphysics 5.5 is used for simulation analysis of the potential differences in the three different states (Figure S1, Supporting Information).

**Performances.** To study the output performance of the GEH-TENG, a linear motor is utilized as the external excitation source. The wave magnitude is mainly determined by characteristic parameters such as wave velocity and wavelength, which are simulated by the frequency and amplitude of the linear motor, respectively. The plane of the guide rail of the linear motor is defined as the water surface. Under conditions in which the angle of the incomplete gear of the GEH-TENG is 80°, the length of the pendulum above the water surface is 80 mm, and the length of the pendulum below the water surface is 60 mm, various experiments described below are performed.

The generation performance of the two generator units working independently at various input frequencies and amplitudes is investigated. The short-circuit current ($I_{SC}$) and


https://doi.org/10.1021/acsnano.1c05685
ACS Nano XXXX, XXX, XXX−XXX

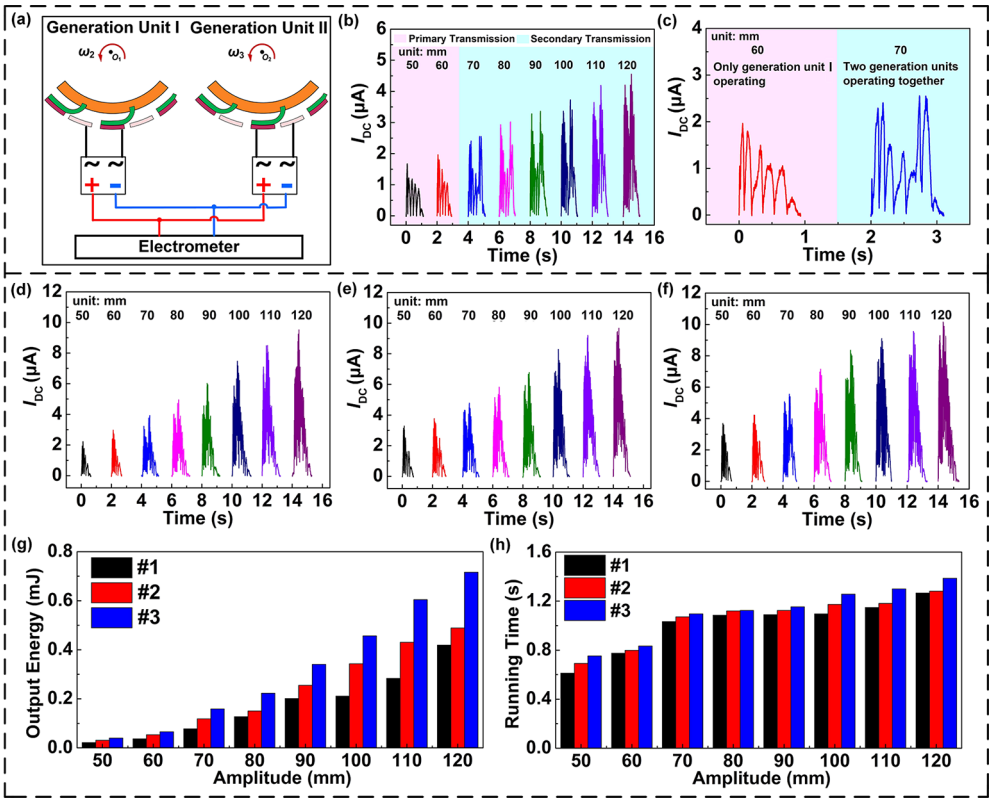


**Figure 4. Operation of two generation units of the GEH-TENG connected in parallel after rectification. (a) Rectification circuit connection diagram. (b, c) Comparison of the $I_{DC}$ output signals under different input amplitudes at 0.5 Hz, and signal amplification and comparison before and after reaching the threshold. The output performance changes with input amplitude under three different counterweight conditions: (d) #1, (e) #2, (f) #3, and (g, h) comparison of output energy and running time of the GEH-TENG in the single operation.**

the direct-current ($I_{DC}$) output (Figure 3a,b) by generation unit I operation changes with the increase of input amplitude when the input frequency is 0.5, 1.0, and 1.5 Hz, respectively. With the constant frequency, the $I_{SC}$, $I_{DC}$, and single running time of the GEH-TENG are gradually increased. Similarly, under the same amplitude, they increase with increasing frequency. Under the same conditions, generation unit II operates separately in the GEH-TENG, and both the $I_{SC}$ and $I_{DC}$ outputs follow similar trends (Figure 3c,d). The difference is that because the swing angle of the pendulum is insufficient when the input amplitude is less than 70 mm, the incomplete gear is unable to drive generation unit II, and hence there is no output signal. Therefore, for the same excitation conditions, in the whole process, the flywheel in the generation unit I continuously rotates, which has a long acceleration time and a long stress time, resulting in a high rotating speed and a large output current. However, the flywheel in the generation unit II only rotates after reaching the threshold value, and the acceleration time is short, resulting in a small output current. Under the same excitation condition, the open-circuit voltage ($V_{OC}$) and the transferred charge ($Q_{SC}$) are obtained (Figure S2, Supporting Information).

To improve the GEH-TENG wave energy harvesting capability, generation units I and II are introduced into the overall structure together (see circuit connection in Figure 4a). The two generation units are connected to two rectifier bridges in series, respectively, and then connected in parallel.

When the input frequency is 0.5 Hz, the $I_{DC}$ output of the GEH-TENG under different input amplitudes (Figure 4b) shows that, when the amplitude is small, the swing angle of the pendulum is small. The GEH-TENG is in the primary transmission state, and only generation unit I engages. When the input amplitude reaches 70 mm, $I_{DC}$ rises again during attenuation, and the peak after rising is higher than the initial peak. This is because at this time, under the action of ambient excitation, the pendulum has swung to an angle that sends the GEH-TENG over the threshold and to enter the secondary transmission state. Generation unit II combines with generation unit I to generate more electricity and thus improve the power generation performance significantly. The $I_{DC}$ output for amplitudes 60 and 70 mm are amplified and compared; the changes in electric signal are evident (Figure 4c). The one-way clutches installed in the gears will be slightly stuck in the process of reverse rotation. On the other hand, the prototype will vibrate slightly during operation, which leads to uneven current attenuation.

Changes in flywheel mass will affect the overall output performance and running time; the mass is determined by the number of equal-mass plates. Therefore, under an external excitation of a fixed frequency of 1.0 Hz, the research is carried out by changing the number of plates in the flywheel of generation units I and II. The mass of each plate is 45 g, by adjusting the number of mass plates in the two flywheels, three different counterweight conditions are set, the cases being labeled #1, #2, and #3, respectively. Details associated with each condition are listed in Table 1.

With the gradual increase in input amplitude, the $I_{DC}$ outputs of the GEH-TENG under three different conditions are shown in Figure 4d–f, respectively. The change in load current across an ambient resistor of 50 MΩ is the same (Figure S3a–c, Supporting Information). The relationship between the three


https://doi.org/10.1021/acsnano.1c05685
ACS Nano XXXX, XXX, XXX−XXX

**Table 1. Three Different Counterweight Conditions**

| counterweight condition | no. of mass plates in the flywheel I (pieces) | no. of mass plates in the flywheel II (pieces) |
|---|---|---|
| #1 | 11 | 15 |
| #2 | 13 | 15 |
| #3 | 15 | 15 |

different conditions and output energy and running time in the single operation under different input amplitudes is obtained (Figure 4g,h). For condition #3, the GEH-TENG has a maximum output energy and the longest running time; in subsequent experiments, both flywheels are therefore set to this condition. When the input frequency increases to 1.5 Hz, for different input amplitudes, changes of $I_{DC}$ and signal amplified images are recorded (Figure S3d–f, Supporting Information).

Furthermore, to study the dependence of the amplitude required to reach the threshold on the intrinsic parameter settings, a series of experiments are performed at a fixed input frequency of 1.0 Hz. In a certain range of input amplitude, the angle of the incomplete gear (Figure 5a,b), length of the pendulum above the water surface (Figure 5d, e), and length of the pendulum below the water surface (Figure 5g,h) of the GEH-TENG are changed, and the output performance is monitored. When the incomplete gear angle is set at 60°, 80°, and 100° successively, with all other parameters kept constant, the input amplitude required to reach the threshold of the GEH-TENG (Figure 5c) is linearly proportional to the increasing incomplete gear angle. It also increases linearly when the length of the pendulum above the water surface increases from 80 mm to 100 mm (Figure 5f).

In addition, the changes in pendulum length below the water surface do not affect the input amplitude required to reach the threshold (Figure 5i). When the length of the pendulum below the water surface is 20 mm, the length of the pendulum is short. The pendulum cannot be pushed by the motor when the input amplitude exceeds 70 mm. Therefore, for this length, the output performance of the GEH-TENG with larger amplitudes is not studied. Under separate input frequencies of 0.5 and 1.5 Hz, the trend is the same (Figures S4 and S5, Supporting Information).

**Demonstration.** To further verify the capability of the GEH-TENG to grade energy, comparative experiments are performed with changes in the condition of generation units in the GEH-TENG at different external excitation frequencies. In the experiment, the angle of the incomplete gear is set to 80°, and the length of the pendulum below and above the wave surface is set to 60 mm and 80 mm, respectively. The change in load current obtained by connecting an ambient resistor of 50 MΩ is obtained (Figure S6, Supporting Information).

Figure 6a shows the output energy of the GEH-TENG at 1.0 Hz under different conditions. When the input amplitude does not reach 70 mm, the GEH-TENG operating with a single generation unit II has no energy output. The output energy of the GEH-TENG with a single generation unit I is the same as that with double generation units. Once the amplitude reaches 70 mm, the output energy of the GEH-TENG with double generation units is more than that with a single generation unit.

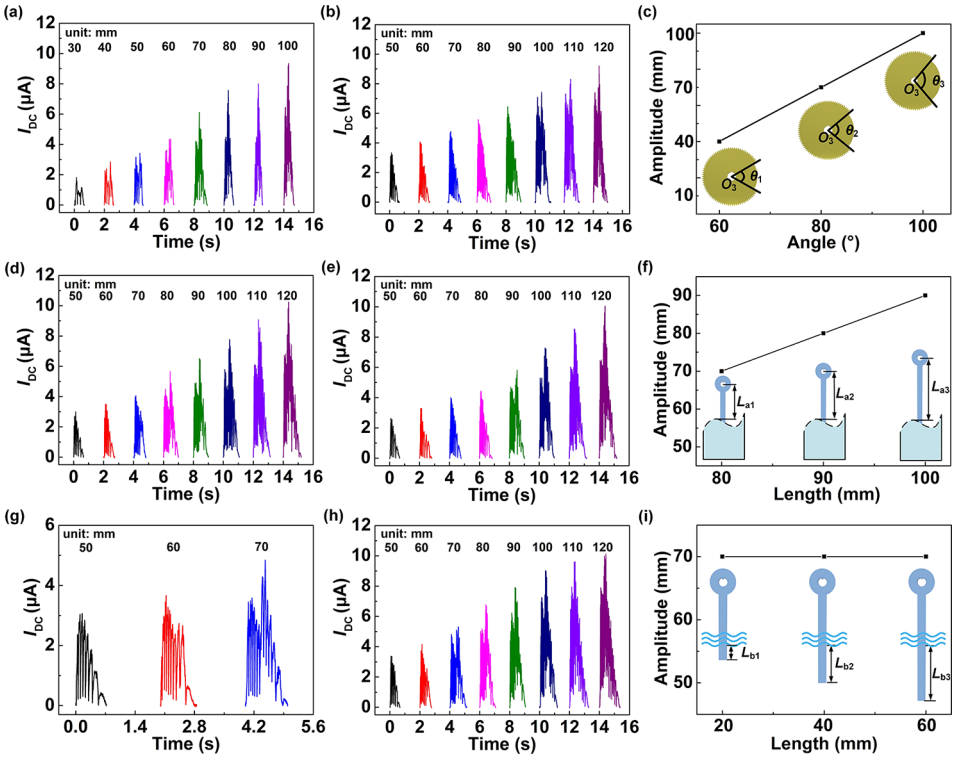


**Figure 5. Output performance of the GEH-TENG under different parameter settings at 1.0 Hz: (a, b) length of the pendulum below the water surface is 60 mm, length of the pendulum above the water surface is 80 mm, and angle of the incomplete gear is 60° and 100°; (d, e) angle of the incomplete gear is 80°, length of the pendulum below the water surface is 60 mm, and length of the pendulum above the water surface is 90 mm and 100 mm; (g, h) angle of the incomplete gear is 80°, length of the pendulum above the water surface is 80 mm, and length of pendulum below the water surface is 20 mm and 40 mm. Comparison of the input amplitudes required to reach threshold under (c) different angles of the incomplete gear, (f) different lengths of the pendulum above the water surface, and (i) different lengths of the pendulum below the water surface.**


https://doi.org/10.1021/acsnano.1c05685
ACS Nano XXXX, XXX, XXX−XXX

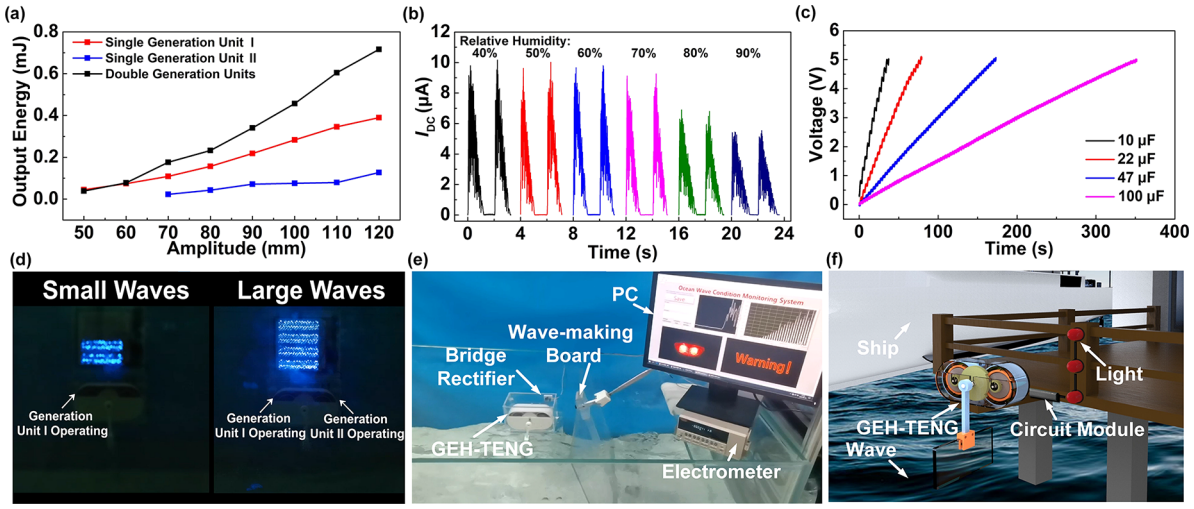


**Figure 6. Electrical characteristics of the GEH-TENG at 1.0 Hz: (a) comparison of output energy of the GEH-TENG under single and double generation units; (b) effect of the environment humidity on $I_{DC}$; (c) voltage of different capacitors charged at a frequency of 1.0 Hz. (d) Lighting LEDs by the GEH-TENG under different ocean wave conditions. (e) Ocean wave condition monitoring by the GEH-TENG. (f) Simulated the GEH-TENG installed on the shore.**

When the amplitude reaches 120 mm, the GEH-TENG with single generation unit I or II can generate 0.3 and 0.12 mJ of energy, respectively, while 0.7 mJ of energy can be generated by the GEH-TENG with double generation units. The energy generated by the GEH-TENG with double generation units can reach 2.3 times that of a single. Output energy at 0.5 and 1.5 Hz frequencies is shown in Figure S7a,b (Supporting Information). A series of experiments prove that under largewave conditions, the GEH-TENG having graded energy harvesting capability, can harvest wave energy more effectively.

Relative humidity of the environment is an important factor affecting the output performance of TENGs. The GEH-TENG is directly exposed to different humidity environments, and performance comparison experiments under different humidity conditions are carried out. The relative humidity of the environment is set to 40−90%, the input amplitude is 120 mm, and the frequency is 1.0 Hz. When the humidity is 40−70%, its output performance decays slowly. When the relative humidity reaches 80−90%, the output performance will quickly decay to 37−52%. Therefore the output performance of the TENG will be adversely affected when the humidity increases sharply. To avoid the influence of humidity, the GEH-TENG can be placed in an acrylic box for sealing in practical application experiments. Under the same external input excitation conditions, the charging of a capacitor by the GEH-TENG device is used to demonstrate the capability of the device (Figure 6c). All voltages of the 10, 22, 47, and 100 $\mu$F capacitors can reach 5 V. The load current of the GEH-TENG under different conditions is measured with different ambient resistors; the peak power is also calculated (Figure S8a−c, Supporting Information). Especially, to prove that the friction materials used by the GEH-TENG still have a good output effect and no obvious damage after long-term operation, a mechanical stability experiment is conducted for one million cycles, which provided support for subsequent practical application (Figure S9, Supporting Information).

To verify its capability in practical applications, a wave simulation test-bed is set up for experiments, and waves are used as external excitation sources. To prevent the damp air and water in the actual environment from corroding the copper and polylactic acid (PLA) materials used in the overall structure of the device, the GEH-TENG is sealed in an acrylic box and placed above the water surface. It continuously operated for 100 000 cycles under the action of waves, which proved its satisfactory durability in the wave environment and the feasibility of the device (Figure S10, Supporting Information). The GEH-TENG employs a series rectifier bridge as a power supply to light LED lamps (Figure 6d, Video S1). With its graded energy harvesting capability, the GEH-TENG enables the monitoring of ocean wave conditions (Figure 6e). When waves are too large, the swing angle of the pendulum reaches the threshold value, and the warning lamp flashes (Video S2). The application experiments prove that the GEH-TENG has wide prospects in the field of ocean wave condition monitoring. In the future, it can be installed on the shore, wharf, and other sites (Figure 6f).

## CONCLUSIONS

In summary, with a graded transmission unit, double generation units, and a pendulum, a graded energy harvesting triboelectric nanogenerator (GEH-TENG) device is fabricated that achieves graded harvesting of wave energy. In smallwave environments, electric energy is generated with one generation unit. The initial torque required is small and easy to start, which can effectively harvest smallwave energy. When the magnitude of the wave increases to make the swing angle of the pendulum reach the preset threshold, it will turn to a double generation units cooperative work state. By adjusting the intrinsic parameters of the GEH-TENG, the input amplitude required to reach the threshold value can be changed, there being a linear relationship between them. Comparative experiments show that this GEH-TENG is capable of generating more electric energy under largewave conditions. The energy generated by the GEH-TENG with double generation units can reach 2.3 times that of a single, and it can charge a 10 $\mu$F capacitor to 5 V within 20 s. In addition, under simulated real-wave environments, ocean wave condition monitoring can be realized according to wave magnitude changes. The concept of graded energy harvesting proposed in this study can be widely used to harvest wave energy


https://doi.org/10.1021/acsnano.1c05685
ACS Nano XXXX, XXX, XXX−XXX

and ocean wave condition monitoring, which provides an idea for the structural design of TENGs.

## EXPERIMENTAL SECTION

**Fabrication of the GEH-TENG.** The triboelectric nanogenerator for graded energy harvesting has dimensions of 230 mm (length) × 100 mm (width) × 110 mm (height). The shell, pendulum, incomplete gear, driven gear I, driven gear II, flywheels, and generation unit shells are all manufactured by 3D printing. The material used in 3D printing is PLA. The lower part of the pendulum is made of acrylic material. All shafts are manufactured by a lathe, and the mass plates are manufactured by using a wire cutter. There are eight FEP films on each flywheel, and each film has a thickness of 100 μm, a width of 40 mm, and a length of 35 mm. Sixteen copper electrodes are uniformly distributed on the inner wall of each generation unit shell.

**Electrical Measurement.** A programmable electrometer (6514, Keithley, USA) and a data acquisition system (PCI-6259, National Instruments, USA) are used to measure and acquire the output signal of the GEH-TENG. External excitation is provided by a linear module (RXP80, RuiXin, China). The wave board is driven by a motor (PL01-19x600/520, LinMot, Switzerland). The temperature and humidity are controlled by an environmental chamber (Y-HF-960L, Aerospace Zhida, China). The collected signals are recorded by LabVIEW.

## ASSOCIATED CONTENT

### Supporting Information

The Supporting Information is available free of charge at https://pubs.acs.org/doi/10.1021/acsnano.1c05685.

Movie S1: Lighting LEDs by the GEH-TENG under different ocean wave conditions (MP4)

Movie S2: Ocean wave condition monitoring by the GEH-TENG (MP4)

Simulations of the device in three states; open-circuit voltage and transferred charge comparison of the GEH-TENG under different input amplitudes and input frequencies; two generation units are connected in parallel after rectification, comparison of output performance under different conditions; output performance of the GEH-TENG under different parameter settings at 0.5 and 1.5 Hz; load current comparison of the GEH-TENG with different input amplitudes; comparison of output energy of the GEH-TENG under single and double generation units at different frequencies; output current and instantaneous output power of the GEH-TENG at different load resistances; performance change of generation unit during continuous operation for one million cycles at 60 rpm; output performance of the GEH-TENG in 100 000 cycles driven by waves (PDF)

## AUTHOR INFORMATION


### Corresponding Authors

**Jianming Wen** − *The Institute of Precision Machinery and Smart Structure, Key Laboratory of Intelligent Operation and Maintenance Technology & Equipment for Urban Rail Transit of Zhejiang Province, College of Engineering, Zhejiang Normal University, Jinhua 321004, China*; Email: wjming@zjnu.cn

**Tinghai Cheng** − *Beijing Institute of Nanoenergy and Nanosystems, Chinese Academy of Sciences, Beijing 101400, China; School of Mechatronic Engineering, Changchun University of Technology, Changchun, Jilin 130012, China; CUSTech Institute of Technology, Wenzhou, Zhejiang 325024, China*; orcid.org/0000-0003-0335-7614; Email: chengtinghai@binn.cas.cn

**Zhong Lin Wang** − *Beijing Institute of Nanoenergy and Nanosystems, Chinese Academy of Sciences, Beijing 101400, China; CUSTech Institute of Technology, Wenzhou, Zhejiang 325024, China; School of Materials Science and Engineering, Georgia Institute of Technology, Atlanta, Georgia 30332-0245, United States*; orcid.org/0000-0002-5530-0380; Email: zhong.wang@mse.gatech.edu

### Authors

**Yuhong Xu** − *Beijing Institute of Nanoenergy and Nanosystems, Chinese Academy of Sciences, Beijing 101400, China; School of Mechatronic Engineering, Changchun University of Technology, Changchun, Jilin 130012, China*

**Weixiong Yang** − *Beijing Institute of Nanoenergy and Nanosystems, Chinese Academy of Sciences, Beijing 101400, China; School of Mechatronic Engineering, Changchun University of Technology, Changchun, Jilin 130012, China*

**Xiaohui Lu** − *School of Mechatronic Engineering, Changchun University of Technology, Changchun, Jilin 130012, China*

**Yanfei Yang** − *Beijing Institute of Nanoenergy and Nanosystems, Chinese Academy of Sciences, Beijing 101400, China*

**Jianping Li** − *The Institute of Precision Machinery and Smart Structure, Key Laboratory of Intelligent Operation and Maintenance Technology & Equipment for Urban Rail Transit of Zhejiang Province, College of Engineering, Zhejiang Normal University, Jinhua 321004, China*

Complete contact information is available at: https://pubs.acs.org/10.1021/acsnano.1c05685

### Author Contributions

⊥Y.X., W.Y., and X.L. contributed equally to this work.


### Notes

The authors declare no competing financial interest.

## ACKNOWLEDGMENTS

The authors are grateful for the support received from the National Key R&D Project from the Minister of Science and Technology (2016YFA0202701 and 2016YFA0202704) and the Beijing Municipal Science and Technology Commission (Z171100002017017).

## REFERENCES


(1) Wang, Z. L.; Song, J. Piezoelectric Nanogenerators Based on Zinc Oxide Nanowire Arrays. *Science* **2006**, *312*, 242−246.

(2) Wang, Z. L.; Jiang, T.; Xu, L. Toward the Blue Energy Dream by Triboelectric Nanogenerator Networks. *Nano Energy* **2017**, *39*, 9−23.

(3) Scruggs, J.; Jacob, P. Harvesting Ocean Wave Energy. *Science* **2009**, *323*, 1176−1178.

(4) Tollefson, J. Power from the Oceans: Blue Energy. *Nature* **2014**, *508*, 302−304.

(5) Tan, J.; Duan, J.; Zhao, Y.; He, B.; Tang, Q. Generators to Harvest Ocean Wave Energy through Electrokinetic Principle. *Nano Energy* **2018**, *48*, 128−133.

(6) Wang, Z. L. Catch Wave Power in Floating Nets. *Nature* **2017**, *542*, 159−160.

(7) Langhamer, O.; Haikonen, K.; Sundberg, J. Wave Power-Sustainable Energy or Environmentally Costly? A Review with Special Emphasis on Linear Wave Energy Converters. *Renewable Sustainable Energy Rev.* **2010**, *14*, 1329−1335.

(8) Wang, T.; Zhang, Y. Design, Analysis, and Evaluation of a Compact Electromagnetic Energy Harvester from Water Flow for Remote Sensors. *Energies* **2018**, *11*, 1424.

(9) Callaway, E. Energy: To Catch a Wave. *Nature* **2007**, *450*, 156−159.
(10) Zhao, J.; Zhen, G.; Liu, G.; Bu, T.; Liu, W.; Fu, X.; Zhang, P.; Zhang, C.; Wang, Z. L. Remarkable Merits of Triboelectric Nanogenerator than Electromagnetic Generator for Harvesting Small-Amplitude Mechanical Energy. *Nano Energy* **2019**, *61*, 111−118.
(11) Sari, I.; Balkan, T.; Külah, H. An Electromagnetic Micro Power Generator for Low-Frequency Environmental Vibrations Based on the Frequency Upconversion Technique. *J. Microelectromech. Syst.* **2010**, *19*, 14−27.
(12) Khan, U.; Kim, S. Triboelectric Nanogenerators for Blue Energy Harvesting. *ACS Nano* **2016**, *10*, 6429−6432.
(13) Falcão, A. Wave Energy Utilization: A Review of the Technologies. *Renewable Sustainable Energy Rev.* **2010**, *14*, 899−918.
(14) Fan, F.; Tian, Z.; Wang, Z. L. Flexible Triboelectric Generator. *Nano Energy* **2012**, *1*, 328−334.
(15) Wang, Z. L. Triboelectric Nanogenerators as New Energy Technology and Self-Powered Sensors-Principles, Problems and Perspectives. *Faraday Discuss.* **2014**, *176*, 447−458.
(16) Zhu, G.; Chen, J.; Zhang, T.; Jing, Q.; Wang, Z. L. Radial-Arrayed Rotary Electrification for High Performance Triboelectric Generator. *Nat. Commun.* **2014**, *5*, 3426.
(17) Zhong, J.; Zhong, Q.; Fan, F.; Zhang, Y.; Wang, S.; Hu, B.; Wang, Z. L.; Zhou, J. Finger Typing Driven Triboelectric Nanogenerator and Its Use for Instantaneously Lighting Up Leds. *Nano Energy* **2013**, *2*, 491−497.
(18) Wang, H.; Jeong, C.; Seo, M.; Joe, D.; Han, J.; Yoon, J.; Lee, K. Performance-Enhanced Triboelectric Nanogenerator Enabled by Wafer-Scale Nanogrates of Multistep Pattern Downscaling. *Nano Energy* **2017**, *35*, 415−423.
(19) Yang, W.; Wang, Y.; Li, Y.; Wang, J.; Cheng, T.; Wang, Z. L. Integrated Flywheel and Spiral Spring Triboelectric Nanogenerator for Improving Energy Harvesting of Intermittent Excitations/Triggering. *Nano Energy* **2019**, *66*, 104104.
(20) Wang, Y.; Yu, X.; Yin, M.; Wang, J.; Gao, Q.; Yu, Y.; Cheng, T.; Wang, Z. L. Gravity Triboelectric Nanogenerator for the Steady Harvesting of Natural Wind Energy. *Nano Energy* **2021**, *82*, 105740.
(21) Chen, J.; Wang, Z. L. Reviving Vibration Energy Harvesting and Self-Powered Sensing by a Triboelectric Nanogenerator. *Joule* **2017**, *1*, 480−521.
(22) Pu, X.; Guo, H.; Tang, Q.; Chen, J.; Feng, L.; Liu, G.; Wang, X.; Xi, Yi.; Hu, C.; Wang, Z. L. Rotation Sensing and Gesture Control of a Robot Joint *via* Triboelectric Quantization Sensor. *Nano Energy* **2018**, *54*, 453−460.
(23) Wang, Z.; Yu, Y.; Wang, Y.; Lu, X.; Cheng, T.; Bao, G.; Wang, Z. L. Magnetic Flap Type Difunctional Sensor for Detecting Pneumatic Flow and Liquid Level Based on Triboelectric Nanogenerator. *ACS Nano* **2020**, *14*, 5981−5987.
(24) Yin, M.; Lu, X.; Qiao, G.; Xu, Y.; Wang, Y.; Cheng, T.; Wang, Z. L. Mechanical Regulation Triboelectric Nanogenerator with Controllable Output Performance for Random Energy Harvesting. *Adv. Energy Mater.* **2020**, *10*, 2000627.
(25) Pang, Y.; Chen, S.; Chu, Y.; Wang, Z. L.; Cao, C. Matryoshka-Inspired Hierarchically Structured Triboelectric Nanogenerators for Wave Energy Harvesting. *Nano Energy* **2019**, *66*, 104131.
(26) Xia, K.; Fu, J.; Xu, Z. Multiple-Frequency High-Output Triboelectric Nanogenerator Based on a Water Balloon for All-Weather Water Wave Energy Harvesting. *Adv. Energy Mater.* **2020**, *10*, 2000426.
(27) Rodrigues, C.; Nunes, D.; Clemente, D.; Mathias, N.; Correia, J.; Rosa-Santos, P.; Taveira-Pinto, F.; Morais, T.; Pereira, A.; Ventura, J. Emerging Triboelectric Nanogenerators for Ocean Wave Energy Harvesting: State of the Art and Future Perspectives. *Energy Environ. Sci.* **2020**, *13*, 2657.
(28) Chen, H.; Xing, C.; Li, Y.; Wang, J.; Xu, Y. Triboelectric Nanogenerators for a Macro-Scale Blue Energy Harvesting and Self-Powered Marine Environmental Monitoring System. *Sustain. Energy Fuels* **2020**, *4*, 1063.
(29) Lei, R.; Shi, Y.; Ding, Y.; Nie, J.; Li, S.; Wang, F.; Zhai, H.; Chen, X.; Wang, Z. L. Sustainable High-Voltage Source Based on Triboelectric Nanogenerator with a Charge Accumulation Strategy. *Energy Environ. Sci.* **2020**, *13*, 2178.
(30) Wang, Z. L. Triboelectric Nanogenerator (TENG)-Sparking an Energy and Sensor Revolution. *Adv. Energy Mater.* **2020**, *10*, 2000137.
(31) Guo, H.; Chen, J.; Wang, L.; Wang, A.; Li, Y.; An, C.; He, J.; Hu, C.; Hsiao, V.; Wang, Z. L. A Highly Efficient Triboelectric Negative Air Ion Generator. *Nat. Sustain.* **2021**, *4*, 147−153.
(32) Xu, C.; Zi, Y.; Wang, A.; Zou, H.; Dai, Y.; He, X.; Wang, P.; Wang, Y.; Feng, P.; Li, D.; Wang, Z. L. On the Electron-Transfer Mechanism in the Contact-Electrification Effect. *Adv. Mater.* **2018**, *30*, 1706790.
(33) Zhu, G.; Zhou, Y.; Bai, P.; Meng, X.; Jing, Q.; Chen, J.; Wang, Z. L. A Shape-Adaptive Thin-Film-Based Approach for 50% High-Efficiency Energy Generation through Micro-Grating Sliding Electrification. *Adv. Mater.* **2014**, *26*, 3788.
(34) Xu, M.; Zhao, T.; Wang, C.; Zhang, S.; Li, Z.; Pan, X.; Wang, Z. L. High Power Density Tower-Like Triboelectric Nanogenerator for Harvesting Arbitrary Directional Water Wave Energy. *ACS Nano* **2019**, *13*, 1932.
(35) Zhu, N.; Kim, Y.; Kim, K.; Shin, B. Change Detection of Ocean Wave Characteristics. *Expert. Syst. Appl.* **2016**, *51*, 245−258.
(36) Wang, Z. L.; Wang, A. On the Origin of Contact-Electrification. *Mater. Today* **2019**, *30*, 34−51.
(37) Davies, D. Charge Generation on Dielectric Surfaces. *J. Phys. D: Appl. Phys.* **1969**, *2*, 1533.


https://doi.org/10.1021/acsnano.1c05685
*ACS Nano* XXXX, XXX, XXX−XXX